

Real non-Hermitian energy spectra without any symmetry

Boxue Zhang(张博学), Qingya Li(李青铓), Xiao Zhang(张笑), and Ching Hua Lee(李庆华)
Citation: Chin. Phys. B, 2022, 31 (**7**): 070308. DOI: 10.1088/1674-1056/ac67c6
Journal homepage: http://cpb.iphy.ac.cn; http://iopscience.iop.org/cpb

What follows is a list of articles you may be interested in

Exact solutions of non-Hermitian chains with asymmetric long-range hopping under specific boundary conditions

Cui-Xian Guo(郭翠仙) and Shu Chen(陈澍)
Chin. Phys. B, 2022, 31 (**1**): 010313. DOI: 10.1088/1674-1056/ac3228

Topological properties of non-Hermitian Creutz ladders

Hui-Qiang Liang(梁辉强) and Linhu Li(李林虎)
Chin. Phys. B, 2022, 31 (**1**): 010310. DOI: 10.1088/1674-1056/ac3991

Two-body exceptional points in open dissipative systems

Peize Ding(丁霈泽) and Wei Yi(易为)
Chin. Phys. B, 2022, 31 (**1**): 010309. DOI: 10.1088/1674-1056/ac3396

Efficient and stable wireless power transfer based on the non-Hermitian physics

Chao Zeng(曾超), Zhiwei Guo(郭志伟), Kejia Zhu(祝可嘉), Caifu Fan(范才富), Guo Li(李果), Jun Jiang(江俊), Yunhui Li(李云辉), Haitao Jiang(江海涛), Yaping Yang(羊亚平), Yong Sun(孙勇), and Hong Chen(陈鸿)
Chin. Phys. B, 2022, 31 (**1**): 010307. DOI: 10.1088/1674-1056/ac3815

Observation of the exceptional point in superconducting qubit with dissipation controlled by parametric modulation

Zhan Wang(王战), Zhongcheng Xiang(相忠诚), Tong Liu(刘桐), Xiaohui Song(宋小会), Pengtao Song(宋鹏涛), Xueyi Guo(郭学仪), Luhong Su(苏鹭红), He Zhang(张贺), Yanjing Du(杜燕京), and Dongning Zheng(郑东宁)
Chin. Phys. B, 2021, 30 (**10**): 100309. DOI: 10.1088/1674-1056/ac0520

SPECIAL TOPIC — Non-Hermitian physics

Real non-Hermitian energy spectra without any symmetry

Boxue Zhang(张博学)[1,†], Qingya Li(李青铓)[2,†], Xiao Zhang(张笑)[1], and Ching Hua Lee(李庆华)[2,‡]

[1] *School of Physics, Sun Yat-sen University, Guangzhou 510275, China*

[2] *Department of Physics, National University of Singapore, Singapore 117542, Singapore*

(Received 4 March 2022; revised manuscript received 5 April 2022; accepted manuscript online 18 April 2022)

Non-Hermitian models with real eigenenergies are highly desirable for their stability. Yet, most of the currently known ones are constrained by symmetries such as PT-symmetry, which is incompatible with realizing some of the most exotic non-Hermitian phenomena. In this work, we investigate how the non-Hermitian skin effect provides an alternative route towards enforcing real spectra and system stability. We showcase, for different classes of energy dispersions, various ansatz models that possess large parameter space regions with real spectra, despite not having any obvious symmetry. These minimal local models can be quickly implemented in non-reciprocal experimental setups such as electrical circuits with operational amplifiers.

Keywords: non-Hermitian physics, real energy spectra, non-Hermitian skin effect

PACS: 03.65.Yz, 03.65.Vf, 03.65.−w **DOI:** 10.1088/1674-1056/ac67c6

1. Introduction

Non-Hermitian systems have recently inspired intense research efforts for their unconventional mathematical properties and physical robustness, such as enlarged topological symmetries,[1–8] exceptional point sensing,[9–15] quantized classical responses,[16] modified bulk–boundary correspondences,[17–32] unconventional entanglement entropy scaling,[4,33–39] enhanced Rabi oscillations,[26,40,41] and effective non-Hermitian curved space.[42,43] Yet, many of these exciting phenomena are often difficult to probe experimentally due to their intrinsically unstable nature from complex eigenenergies. While real eigenenergies can be symmetry-enforced, i.e., through PT-symmetry,[44–51] doing so is incompatible with realizing many of the most exotic non-Hermitian phenomena.[20,52–66]

In this work, we carefully investigate how the non-Hermitian skin effect (NHSE)[67–73] can also enforce real non-Hermitian spectra, even for lattices whose couplings and momentum-space descriptions do not admit any obvious symmetry. The NHSE has been heavily associated with modified bulk-boundary correspondences[17,39] and, in our context, implies that a system can robustly possess real spectrum in the presence of a boundary, even though its bulk is unstable with complex eigenenergies. Physically, this is because the directed amplification in a NHSE lattice can be stabilized by the interfering wavepackets from a boundary or spatial inhomogeneity, a mechanism that is unrelated to conventional symmetry protection.

We elucidate this route towards real eigenspectra in terms of the inverse skin depth[17,74] κ, which is an additional degree of freedom that mathematically takes the role of imaginary momentum. It physically controls the accumulation and interference of skin states at a boundary, and mathematically replaces the Bloch description of the lattice by an effective surrogate[74] model that can look completely different. Specifically, we shall show that in a bounded lattice, the reality of the spectrum is only destroyed by a spontaneous symmetry breaking process that can occur much later than the explicit symmetry breaking at the Bloch level.

2. OBC vs. PBC spectra

We first review and distinguish the approaches for computing the eigenenergy spectrum under open vs. periodic boundary conditions (OBCs vs. PBCs). Given a generic non-Hermitian Hamiltonian $H(k)$, PBC eigenenergies $\tilde{E}$ and OBC eigenenergies $\bar{E}$ are obtained very differently. To find the set of $E \in \tilde{E}$, we simply solve for eigenenergies E such that characteristic polynomial $P(E,k) = \mathrm{Det}[H(k) - E\mathbb{I}] = 0$, where $k \in [0, 2\pi)$. However, under OBCs, translation invariance is broken, and in general the spectrum is not indexed by real momentum k. Instead, the OBC spectrum $E \in \bar{E}$ is given by eigenenergies E that solve

$$P(p) = P(E, k + \mathrm{i}\kappa) = \mathrm{Det}[H(k + \mathrm{i}\kappa) - E\mathbb{I}] = 0 \quad (1)$$

and are degenerate in both E and κ. Here κ is the imaginary part of the complexified momentum $p = k + \mathrm{i}\kappa$ that also represents the inverse decay length (skin depth) of eigenstates viz. $\mathrm{e}^{\mathrm{i}px} \sim \mathrm{e}^{-\kappa x}$, i.e., taking the role of a length scale[75,76] not present in Hermitian systems. This κ degeneracy is re-

[†] These authors contributed equally.

[‡] Corresponding author. E-mail: phylch@nus.edu.sg

© 2022 Chinese Physical Society and IOP Publishing Ltd

quired because OBC skin eigenstates have exponential spatial profiles, and we need a superposition of two of them with identical E and κ to satisfy OBCs at two arbitrarily separated boundaries (as we interpolate between OBCs and PBCs, we observe a peculiar scaling behavior of the corresponding effective κ[98]). In general, we write $\kappa = \kappa(k)$ to emphasize its k-dependence, and $p = k + \mathrm{i}\kappa(k)$ is known as the generalized Brillouin zone (GBZ).[17,18,18,19,21–23,78] $H(p) = H(k + \mathrm{i}\kappa(k))$ is also referred to as the surrogate Hamiltonian, which is used instead of the original Bloch Hamiltonian $H(k)$ in computing topological invariants (however, the topological eigenenergies themselves fall outside of the purview of our prescription, because they are isolated solutions that are not adiabatically connected to any Bloch solution)[80–82] and spectral properties under OBCs.

Note that the above prescriptions for the OBC and PBC eigenenergies cocide in the case of Hermitian lattices, since as p cycles through real values $[0, 2\pi)$, every value of E lies on the real line and will be visited at least twice, both with $\kappa = \mathrm{Im}(p) = 0$.

2.1. Minimal model with different OBC vs. PBC spectra

As a concrete demonstration, we consider a minimal model with $H_{\mathrm{min}}(z) = z + \frac{1}{z} + Az^2$, where $z = \mathrm{e}^{\mathrm{i}k}$. In real space, it contains two symmetric nearest neighbor (NN) hoppings and another uncompensated next-nearest-neighbor (NNN) hopping: $H_{\mathrm{min}} = \sum_x |x+1\rangle\langle x| + |x\rangle\langle x+1| + A|x+2\rangle\langle x|$. Clearly, its PBC spectrum is given by $\tilde{E} = 2\cos k + A\mathrm{e}^{2\mathrm{i}k}$, and is entirely complex unless $A = 0$, as plotted as the thick red curve in Fig. 1 for $A = 2$. However, large segments of its OBC spectrum lie on the real line, as shown by the black dots.

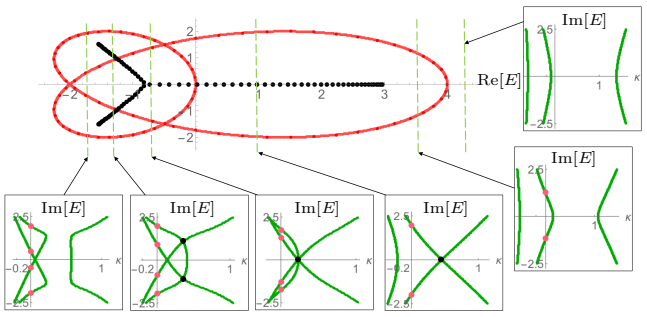


Fig. 1. Real OBC vs. real PBC spectra in terms of the symmetry of $\kappa(E)$ solutions. Shown are the OBC (black) and PBC (red) spectra of the model H_{min} with dispersion $E(z) = z + z^{-1} + 2z^2$; the inset plots show $\mathrm{Im}(E(z))$ as a function of $\kappa = -\log|z|$ (green κ curves) at various fixed $\mathrm{Re}(E(z))$ slices. PBC eigenenergies (red dots) correspond to $(\mathrm{Re}(E(z)), \mathrm{Im}(E(z)))$ consistent with $\kappa = 0$, and OBC eigenenergies (black dots) correspond degeneracies in both κ and $E(z)$ (green curve intersections). In particular, we have real OBC eigenenergies when the green curves intersect at $\mathrm{Im}(E) = 0$, which often occurs even when the PBC eigenenergies are non-real.

Below, we explain how one can visually derive the OBC and PBC spectra. We turn to the plots of κ solutions vs. $\mathrm{Im}(E)$, for fixed $\mathrm{Re}(E)$ slices. Going from large to small $\mathrm{Re}(E)$, we find that PBC eigenenergies (red) first appear when we pass $\mathrm{Re}(E) = 4$, followed by OBC eigenenergies (black) after $\mathrm{Re}(E) = 3$. In the green $\mathrm{Im}(E)$ vs. κ plots, it is apparent that PBC eigenenergies appear when the green κ solution curves cross $\kappa = 0$, while OBC eigenenergies only appear when the κ curves intersect. This is exactly what was prescribed earlier $-\kappa = 0$ gives the PBC spectrum, while κ degeneracies give the OBC spectrum. As $\mathrm{Re}(E)$ decreases further, additional PBC winding loops appear, and they correspond to additional 0 crossings of κ from the green curve that is emerging from small κ. At $\mathrm{Re}(E) \approx -0.79$, that green curve goes over the original black κ intersection, thereby splitting it into two black intersections. That corresponds to the two black OBC branches away from the real E line. Finally, when these two κ intersections gap out at sufficiently negative $\mathrm{Re}(E)$, the OBC eigenenergies disappear.

All in all, we see that real OBC eigenenergies correspond to intersections of the κ curves at $\mathrm{Im}(E) = 0$, which can exist even if PBC eigenenergies are already complex, i.e., if the κ curves cross $\kappa = 0$ at $\mathrm{Im}(E) \neq 0$. As such, the breakdown of the reality of the spectra can be understood as the breaking of the symmetry of the κ curves. In the following we detail the conditions to have non-real PBC and OBC spectrum, and it is clear that the later is often harder to achieve. While a non-real PBC spectrum only requires the κ curves to have asymmetric zero crossings, which are almost guaranteed in a system without PT symmetry, a non-real OBC spectrum requires that symmetry to be spontaneously broken, i.e., broken at the level of "extrema" corresponding to the intersection points. Tellingly, it is often much harder to have asymmetric κ intersections rather than κ zero crossings, and that explains the relative robustness of real OBC spectra compared to real PBC spectra.

3. Parameter spaces for real eigenenergies

We next present the parameter space for real OBC spectra for several paradigmatic models. It has to be emphasized that almost all eigenenergies (under both OBCs and PBCs) fundamentally depend on the form of the dispersion $P(E, p)$, and only indirectly on the form of the Hamiltonian. The exceptions are the eigenenergies of isolated topological modes, which are protected by bulk eigenstate topology, but we will not focus on them here.

An important simplifying symmetry for OBC (but not PBC) spectra is its invariance under constant translations of κ, i.e., $H(p)$ and $H(p + \mathrm{i}\kappa_0)$ always possess identical OBC spectra for any fixed κ_0. This is because the OBC spectra are determined by κ crossings, which are unaffected by overall translations. As such, each model belongs to an equivalence class of models related by hopping rescalings, all possessing the same OBC spectrum. As an illustration, $H_{\mathrm{min}}(z) = z + \frac{1}{z} + Az^2$ has

identical OBC spectrum as $H'_{\rm min}(z)=\mathrm{e}^{-\kappa_0}z+\frac{\mathrm{e}^{\kappa_0}}{z}+A\,\mathrm{e}^{-2\kappa_0}z^2$, for which the $A=0$ case reduces to the famed Hatano–Nelson model with unequal NN couplings.[29,83,84]

3.1. Separable energy dispersions *P(E, p)*

We first discuss separable dispersions, namely, those with $P(E,p)=F(E)+G(p)$, where $F(E)$ is a function of E and $G(p)$ is a Laurent polynomial of $z=\mathrm{e}^{\mathrm{i}p}$. As long as $G(p)$ gives an OBC spectral curve that does not contain branches, we can in principle achieve a real spectrum by modifying the model such that $F(E)$ conformally[85] maps the curve onto the real line. For this reason, the non-Hermitian SSH model and its variants can all possess real spectra.[17,85,86]

3.1.1. Single-component Hamiltonians

We start with the single-component Hamiltonians, whose characteristic polynomials are simply given by $P(E,p)=H(p)-E$. As discussed above, cases with only two NN hoppings are trivial, since they are always reducible to the equivalence class of $H(z)=z+z^{-1}$. As such, the minimal nontrivial case is the 3-hoppings model $H_{\rm min}(z)$, which we just examined. There are two ways to generalize to the next level of sophistication through a fourth hopping term, namely,

$$H^1_{\text{1-band}}(z)=z+\frac{1}{z}+Az^2+Bz^3, \tag{2}$$

$$H^2_{\text{1-band}}(z)=z+\frac{1}{z}+Az^2+\frac{1}{z^2}B, \tag{3}$$

where $z=\mathrm{e}^{\mathrm{i}p}$. These two models capture all the possibilities for Hamiltonians with hoppings spanning four sites, up to reflection and translation symmetry. Note that for single-component models, the onsite term is just a trivial constant. Also, all meaningful models must possess both left and right hoppings, since otherwise the OBC spectrum will collapse onto a single point.[87,88]

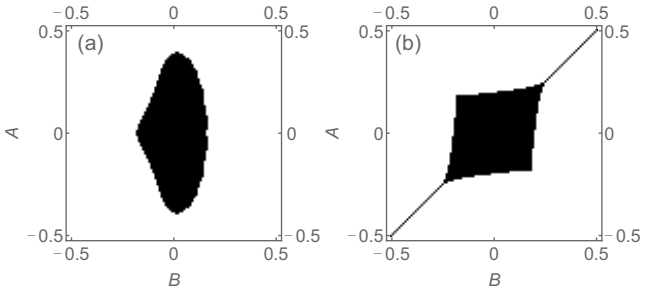


Fig. 2. Regions of the parameter space with real OBC spectra (black) for the following 2-component models: (a) $H^1_{\text{1-band}}$ and (b) $H^2_{\text{1-band}}$. In (b), models with $A=B$ also trivially result in real spectra. The numerical threshold is $\mathrm{Max}|\mathrm{Im}(E)|<\varepsilon=10^{-6}$.

As we can see from Figs. 2(a) and 2(b), there exists a rather large (black) region in the (A,B) parameter space where the spectra still remain real, despite A and B manifestly breaking any possible symmetry. Indeed, the Az^2+Bz^3 term of $H^1_{\text{1-band}}(z)$ gives rise to robustly complex eigenenergies under PBCs, even though it can still give a real spectrum for A as large as 0.35 (Fig. 2(a)). For $H^2_{\text{1-band}}(z)$ with dispersion $2\cos p+A\,\mathrm{e}^{2\mathrm{i}p}+B\,\mathrm{e}^{-2\mathrm{i}p}$, the OBC spectrum is trivially real for $A=B$, but still remains real for a large parameter region away from that (Fig. 2(b)). Physically, this is so because interference from waves reflected off a boundary are sufficient in preventing a wavepacket from being amplified indefinitely.

3.1.2. Two-component Hamiltonians

In 2-band models, we have

$$P_2(E,p)=E^2-[\mathrm{Tr}H_2(p)]E+\mathrm{Det}H_2(p), \tag{4}$$

such that separable dispersions correspond to Hamiltonians with p-independent traces, which can occur when the diagonal terms are either zero or constant. Physically, this corresponds to the absence of homogeneous same-sublattice net hoppings across different unit cells.

In this case of constant trace, the dispersion is essentially determined by $F(E)=-G(p)=\mathrm{Det}H_2(p)$, directly generalizing the case of 1-component models upon the conformal transform $E\to E^2-[\mathrm{Tr}H_2]E$. The only difference is that $G(p)$ now contains products of matrix elements of $H_2(p)$, and as such is usually a higher-order polynomial describing OBC spectra with no analytic solution. While a higher-order $G(p)$ can result in a more branched and hence complex OBC spectrum, with appropriate model design, there can still be larger parameter regions with real OBC spectra, see Fig. 3.

For instructive purposes, we first study the 2-component model with almost trivial NHSE:

$$H^0_{\text{2-band}}(z)=\left(z+Az^{-1}\right)\sigma_x+B\sigma_y, \tag{5}$$

where σ_x and σ_y are the Pauli matrices. Upon performing the κ_0 translation $p\to p+\mathrm{i}\,\kappa_0=p+\mathrm{i}\log\sqrt{A}$, we find the dispersion $E^2=-G(p)=B^2+2A\cos 2p$. As such, the spectrum is real whenever $B^2>-2A$, as numerically verified in Fig. 3(a).

Next, inspired by the 1-component cases, we present the following models with nontrivial real spectral parameter regions:

$$H^1_{\text{2-band}}(z)=\left(Az^2+\frac{1}{z}+C\right)\sigma_+ +\left(z+\frac{B}{z^2}+D\right)\sigma_-, \tag{6}$$

$$H^2_{\text{2-band}}(z)=\left(Az^2+\frac{1}{z}+C\right)\sigma_+ +\left(z+Bz^3+D\right)\sigma_-, \tag{7}$$

$$H^3_{\text{2-band}}(z)=\left(\frac{A}{z^2}+\frac{1}{z}+C\right)\sigma_+ +\left(z+\frac{B}{z^3}+D\right)\sigma_-, \tag{8}$$

where $\sigma_\pm=(\sigma_x\pm\mathrm{i}\,\sigma_y)/2$ and $z=\mathrm{e}^{\mathrm{i}p}$. In these models, the hoppings are different in either direction, and it is surprising from Figs. 3(b)–3(h) that real OBC spectra not just exist, but in fact over large parameter space regions. For instance, in $H^2_{\text{2-band}}$ with $C=2,D=1$ (Fig. 3(h)), the OBC spectrum can be real even for $A>1$, which corresponds to a very unbalanced set of physical couplings.

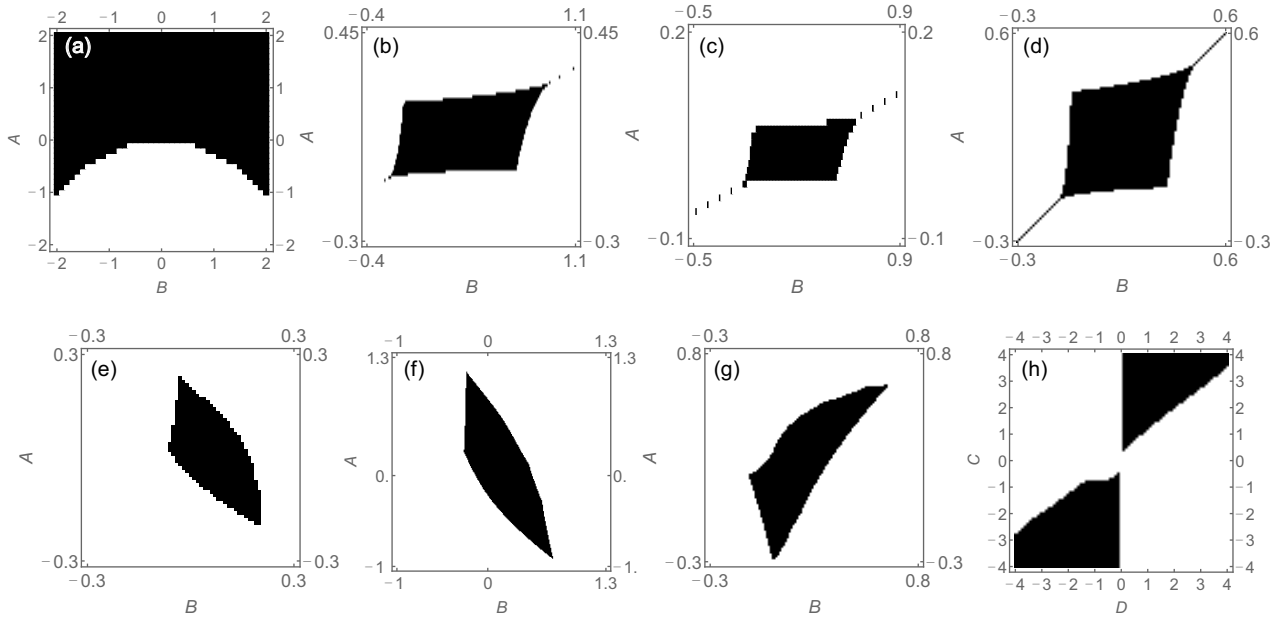


Fig. 3. Regions of the parameter space with real OBC spectra (black) for the following 2-component separable models: (a) $H^0_{\text{2-band}}$; (b) $H^1_{\text{2-band}}$ with $C=2,D=3$; (c) $H^1_{\text{2-band}}$ with $C=1/2,D=1$; (d) $H^1_{\text{2-band}}$ with $C=2,D=2$; (e) $H^2_{\text{2-band}}$ with $C=2,D=3$; (f) $H^2_{\text{2-band}}$ with $C=2,D=1$; (g) $H^3_{\text{2-band}}$ with $C=2,D=2$; (h) $H^3_{\text{2-band}}$ with $A=0.1,B=0.1$. The numerical threshold is $\text{Max}|\text{Im}(E)|<\varepsilon=10^{-6}$. Note that the PBC spectra of all of these models are complex.

3.2. Inseparable energy dispersions *P(E, p)*

We next consider more sophisticated dispersions which contain products of E and $z=\mathrm{e}^{\mathrm{i}k}$. In general, they are not analytically tractable, although their spectral graph structure can often still be heuristically predicted.[85] In this work, we shall limit ourselves to 2-component models. From Eq. (4), those with inseparable dispersions correspond to those with p-dependent traces, i.e., those with same-sublattice hoppings across unit cells.

3.2.1. Analytically tractable examples

First, we introduce an inseparable case whose condition for real spectrum can still be analytically derived. Consider

$$H^1_{\text{in}}(z)=\begin{pmatrix} Az^3 & \sqrt{C} \\ \sqrt{C} & B/z^3 \end{pmatrix} \tag{9}$$

with dispersion given by the characteristic polynomial

$$P^1_{\text{in}}(E,z)=E^2-\left(Az^3+\frac{B}{z^3}\right)E+AB-C, \tag{10}$$

where $z=\mathrm{e}^{\mathrm{i}p}$. To make analytic headway, we perform the hopping rescaling $p\to p+\mathrm{i}\log\sqrt[6]{A/B}$ so as to symmetrize the Az^3+Bz^{-3} term to $\sqrt{AB}(z^3+z^{-3})$. Doing so does not change the OBC spectrum; yet, due to the symmetric occurrence of z and z^{-1}, we also know that $\kappa=0$, i.e., real p constitutes a potential solution for the OBC spectrum. Whether real p indeed generates the correct solution depends on whether a competing degenerate κ solution exists. For this model, it is not hard to show that, with $p\to\mathrm{i}\log\sqrt[6]{B/A}$,

$$\begin{aligned} P^1_{\text{in}}(E,z) &= E^2-2\sqrt{AB}E\cos 3p+AB-C \\ &= \left(E-\sqrt{AB}\cos 3p\right)^2+AB\sin^2 3p-C=0 \end{aligned} \tag{11}$$

admits real E solutions generated by real p as long as $0\le AB\le C$. Outside of this regime, complex pairs of E solutions appear (Fig. 4(a)), leading to non-real spectra. Figure S1 shows the boundary behaviour of spectra from real to non-real as the parameter varies. This criterion $0\le AB\le C$ entails that the real spectrum hinges on the presence of nonzero coupling, and is numerically verified in Fig. 4(a).

Next, we introduce another Hamiltonian which admits real spectrum for parameters that make it separable:

$$H^2_{\text{in}}(z)=\begin{pmatrix} Az & 1+z^2 \\ 2+1/z^2 & Bz \end{pmatrix} \tag{12}$$

with

$$P^2_{\text{in}}(E,z)=E^2-(A+B)Ez+(AB-2)z^2-3-z^{-2}. \tag{13}$$

Although its GBZ and thus OBC spectrum are not analytically solvable for general parameters, for the special case when $A=-B$, the trace term disappears, and we simply obtain $E=\pm\sqrt{(2+A^2)z^2+z^{-2}+3}$. Again, this is of Hatano–Nelson form, and setting $p\to p+\mathrm{i}\log\sqrt[4]{2+A^2}$, we obtain $\bar{E}=\pm\sqrt{3+2\sqrt{2+A^2}\cos 2p}$. This is real for $A=-B$ with $|A|<1/2$, as reflected in its numerical parameter space diagram (Fig. 4(b)).

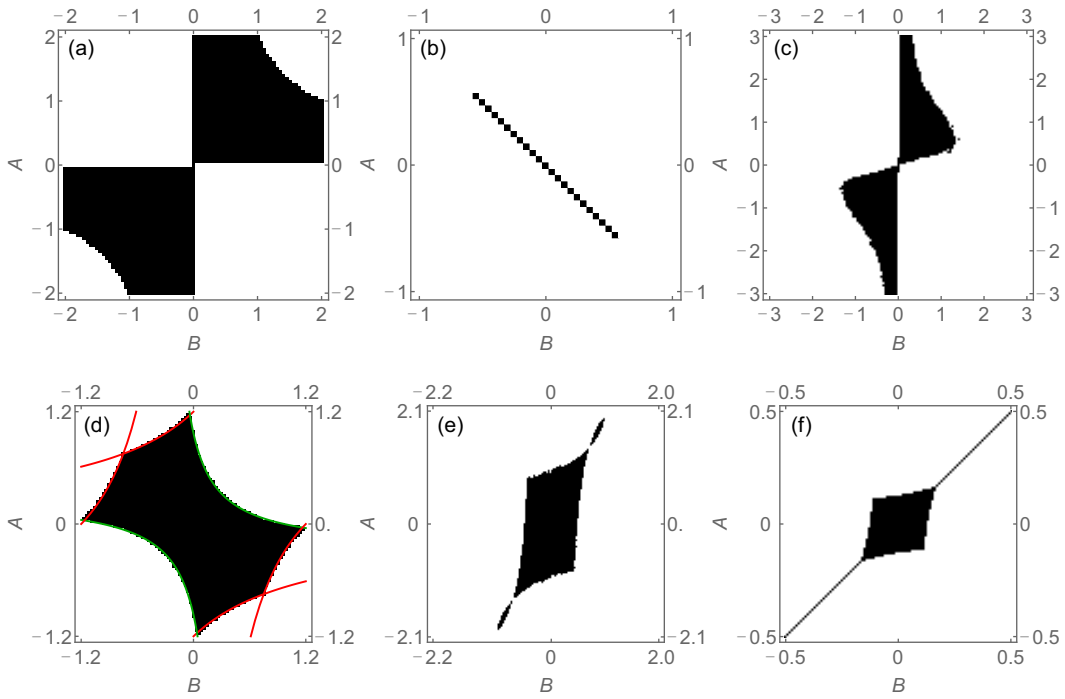


Fig. 4. Regions of the parameter space with real OBC spectra (black) for the following 2-component inseparable models: (a) $H^1_{\rm in}(z)$; (b) $H^2_{\rm in}(z)$; (c) $H^3_{\rm in}(z)$; (d) $H^4_{\rm in}(z)$ with the regime boundary approximately depicted by curves $(0.28+A)(0.28+B)=0.35$ and its reflection across line $A=-B$ (green), $1.2=A(-0.8B+1)$ and its reflection across line $A=-B$ plus further reflection across line $A=B$ (red); (e) $H^5_{\rm in}(z)$; (f) $H^6_{\rm in}(z)$. The system length is $L=30$ for all and the numerical threshold is $\mathrm{Max}|\mathrm{Im}(E)|<\varepsilon$, where $\varepsilon=10^{-5}$ for (c) and $\varepsilon=10^{-6}$ for the other cases.

3.2.2. More general examples

Next, we introduce a few more models whose propensity for real OBC spectra cannot be predicted through any simple way:

$$H^3_{\rm in}(z)=\begin{pmatrix}2+Az & 2\\ 1 & 1+B/z\end{pmatrix}, \tag{14}$$

$$H^4_{\rm in}(z)=\begin{pmatrix}1+Az & 1+z\\ 2+1/z & 1+Bz\end{pmatrix}, \tag{15}$$

$$H^5_{\rm in}(z)=\begin{pmatrix}Az & 1+z\\ 2+1/z & B/z\end{pmatrix}, \tag{16}$$

$$H^6_{\rm in}(z)=\begin{pmatrix}z+Az^2 & 2\\ 1 & 1/z+B/z^2\end{pmatrix}. \tag{17}$$

Like $H^1_{\rm in}$ of Eq. (9), the model $H^3_{\rm in}$ contains constant off-diagonal couplings. However, despite its simple algebraic form, it is not analytically tractable, and in fact behaviors completely differently from $H^1_{\rm in}$, and in fact the other models too.

The real spectrum parameter region of $H^6_{\rm in}$ is an interesting intersection of a diagonal $A=B$ line segment, and a smaller extended region. These two parameter subregions have different origins. For the former, the OBC spectrum is real because the PBC spectrum is also real; larger $A=B$ closes the band gap and releases complex eigenenergies. For the latter, the PBC spectrum is always complex (example in Fig. S2), but an open boundary creates sufficient interference to stop indefinite amplification, leading to a completely real spectrum.

4. Discussion

In this work, we have seen that real non-Hermitian OBC spectra are generically more robust than real PBC spectra. This can be explained in terms of the inverse skin depth $\kappa(E)$ solutions curves — while the PBC spectrum becomes complex once $\kappa(E)\neq 0$ at $\mathrm{Im}E\neq 0$, a complex OBC spectrum requires $\kappa(E)$ curves to intersect at $\mathrm{Im}E\neq 0$, which is a more demanding condition. While there exists a very general electrostatics approach[89] that returns possible parent Hamiltonians for any desired real OBC spectrum and skin localization, this work showcases particularly simple ansatz models that have the benefit of being as local as possible.

The discovery of these Hamiltonians with real spectra complements existing efforts towards the design of stable non-Hermitian system, particularly the PT-symmetry route. With a greater set of ansatze models that are not symmetry constrained, a larger variety of interesting non-Hermitian physics, i.e., non-Hermitian skin clusters and pseudogaps[90–92] can be realized not just with enhanced stability, but also with generically non-reciprocal platforms such as circuits with MOSFETs or operational amplifiers.[20,46,59,93–97] Yet, the NHSE is not guaranteed to yield real spectra, and in Appendix A, we have also listed down models which failed, to aid further search efforts.

Appendix A: Inseparable energy dispersions not giving real spectra

While the main text had discussed various models with real spectra despite having no favorable symmetries, it is also important to record models where thisdoes not occur. As discussed, NHSE-induced real spectra depend on the algebraic properties of the $\kappa(E)$ curves, and it is instructive to list the models where they do not behave favorably as such.

For instance, the following deformations of $H^1_{\rm in}(z)$ have no real spectra:

- $H^1_{\rm in,m1}(z)=\begin{pmatrix} Az^n & 0 \\ c_1 & Bz^{-n}\end{pmatrix}$,
- $H^1_{\rm in,m2}(z)=\begin{pmatrix} Az^n & -c_1 \\ c_1 & Bz^{-n}\end{pmatrix}$, for sufficiently small c_1, which is expected as they do not fulfil the condition of $0\leq AB\leq C$, where $C=0$ for $H^1_{\rm in,m1}$ and $C=c_1^2$ for $H^1_{\rm in,m2}$.
- $H^1_{\rm in,m3}(z)=\begin{pmatrix} Az^n & 0 \\ c_1 & Bz^n\end{pmatrix}$.

Modifications of $H^2_{\rm in}(z)$ and $H^4_{\rm in}(z)$ with diagonal terms having all positive powers of z only:

- $H^4_{\rm in,m1}(z)=\begin{pmatrix} 1+Az & 1+z \\ 2+z & 1+Bz\end{pmatrix}$.

Modifications of $H^3_{\rm in}(z)$ with diagonal terms having the same sign of power of z:

- by having the same sign of power of z at the non-diagonal terms

$$H^3_{\rm in,m1}(z)=\begin{pmatrix} 2+Az & c_2 \\ 1 & 1+Bz\end{pmatrix},\ \text{with } c_2=1,-1,0.$$

Modifications of $H^5_{\rm in}(z)$ with diagonal terms having positive and negative powers of z:

- $H^5_{\rm in,m1}(z)=\begin{pmatrix} Az & 1+z^2 \\ 2+z^{-2} & Bz^{-1}\end{pmatrix}$,
- by having the same sign of power of z at the non-diagonal terms

$$H^5_{\rm in,m2}(z)=\begin{pmatrix} Az & 1+z \\ 2+z & Bz^{-1}\end{pmatrix}.$$

Modifications of $H^6_{\rm in}(z)$ with diagonal terms having the same sign of power of z:

- $H^6_{\rm in,m1}(z)=\begin{pmatrix} 1+z+Az^2 & 1 \\ 2 & 1+z+Bz^{-2}\end{pmatrix}$,

$H^6_{\rm in,m2}(z)=\begin{pmatrix} 1+z+Az^2 & 1 \\ 2 & 1+z^{-1}+Bz^2\end{pmatrix}$.

Models with non-symmetric hopping systems:

- $H_{\rm c1}(z)=\begin{pmatrix} Az^2 & z \\ 2 & Bz^{-2}\end{pmatrix}$,
- $H_{\rm c2}(z)=\begin{pmatrix} Az^2 & z \\ 2 & Bz^{2}\end{pmatrix}$,
- $H_{\rm c3}(z)=\begin{pmatrix} Az^2 & z+2 \\ 2 & Bz^{-2}\end{pmatrix}$,
- $H_{\rm c4}(z)=\begin{pmatrix} Az^2 & z+2 \\ 2 & z^{-1}+Bz^{-2}\end{pmatrix}$,
- $H_{\rm c5}(z)=\begin{pmatrix} 1+z+Az^2 & 2 \\ 2 & Bz^{-2}\end{pmatrix}$.

Acknowledgments

X.Z. is supported by the National Natural Science Foundation of China (Grant No. 11874431), the National Key R&D Program of China (Grant No. 2018YFA0306800), and the Guangdong Science and Technology Innovation Youth Talent Program (Grant No. 2016TQ03X688).

References

[1] Kawabata K, Shiozaki K, Ueda M and Sato M 2019 *Phys. Rev. X* **9** 041015
[2] Liu C H, Jiang H and Chen S 2019 *Phys. Rev. B* **99** 125103
[3] Bergholtz E J, Budich J C and Kunst F K 2021 *Rev. Mod. Phys.* **93** 015005
[4] Sayyad S, Yu J, Grushin A G and Sieberer L M 2021 *Phys. Rev. Res.* **3** 033022
[5] Wojcik C C, Wang K, Dutt A, Zhong J and Fan S 2021 arXiv preprint arXiv: 2111.09977
[6] Shiozaki K and Ono S 2021 *Phys. Rev. B* **104** 035424
[7] Borgnia D S, Kruchkov A J and Slager R J 2020 *Phys. Rev. Lett.* **124** 056802
[8] Park H, Gao W, Zhang X and Oh S S 2022 *Nanophotonics*
[9] Chen W, Özdemir Ş, Zhao G, Wiersig J and Yang L 2017 *Nature* **548** 192
[10] Wiersig J 2014 *Phys. Rev. Lett.* **112** 203901
[11] Zhang M, Sweeney W, Hsu C W, Yang L, Stone A D and Jiang L 2019 *Phys. Rev. Lett.* **123** 180501
[12] Zeng C, Sun Y, Li G, Li Y, Jiang H, Yang Y and Chen H 2019 *Opt. Express* **27** 27562
[13] Budich J C and Bergholtz E J 2020 *Phys. Rev. Lett.* **125** 180403
[14] Sahoo A and Sarma A K 2022 arXiv preprint arXiv: 2202.07972
[15] Hodaei H, Hassan A U, Wittek S, Garcia-Gracia H, El-Ganainy R, Christodoulides D N and Khajavikhan M 2017 *Nature* **548** 187
[16] Li L, Mu S, Lee C H and Gong J 2021 *Nat. Commun.* **12** 5294
[17] Yao S and Wang Z 2018 *Phys. Rev. Lett.* **121** 086803
[18] Yang Z, Zhang K, Fang C and Hu J 2020 *Phys. Rev. Lett.* **125** 226402
[19] Yokomizo K and Murakami S 2019 *Phys. Rev. Lett.* **123** 066404
[20] Helbig T, Hofmann T, Imhof S, Abdelghany M, Kiessling T, Molenkamp L, Lee C, Szameit A, Greiter M and Thomale R 2020 *Nat. Phys.* **16** 747
[21] Yao S, Song F and Wang Z 2018 *Phys. Rev. Lett.* **121** 136802
[22] Zhang K, Yang Z and Fang C 2020 *Phys. Rev. Lett.* **125** 126402
[23] Guo G F, Bao X X and Tan L 2021 arXiv preprint arXiv: 2106.06384
[24] Bartlett J, Hu H and Zhao E 2021 *Phys. Rev. B* **104** 195131
[25] Zhang Z Q, Liu H, Liu H, Jiang H and Xie X C 2022 arXiv preprint arXiv: 2201.01577
[26] Cao Y, Li Y and Yang X 2021 *Phys. Rev. B* **103** 075126
[27] Jin L and Song Z 2019 *Phys. Rev. B* **99** 081103
[28] Kunst F K, Edvardsson E, Budich J C and Bergholtz E J 2018 *Phys. Rev. Lett.* **121** 026808
[29] Koch R and Budich J C 2020 *Eur. Phys. J. D* **74** 70
[30] Imura K I and Takane Y 2020 *Prog. Theor. Exp. Phys.* **2020** 12A103

[31] Qin F, Shen R and Lee C H 2022 arXiv preprint arXiv: 2202.10481
[32] Jiang H and Lee C H Jiang H and Lee C H 2022 *Chin. Phys. B* **31** 050307
[33] Li L, Lee C H, Mu S and Gong J 2020 *Nat. Commun.* **11** 5491
[34] Lee C H 2022 *Phys. Rev. Lett.* **128** 010402
[35] Chen W, Peng L, Lu H and Lu X 2022 *Phys. Rev. B* **105** 075126
[36] Chang P Y, You J S, Wen X and Ryu S 2020 *Phys. Rev. Res.* **2** 033069
[37] Zhou B, Wang R and Wang B 2020 *Phys. Rev. B* **102** 205116
[38] Yokomizo K and Murakami S 2021 *Phys. Rev. B* **104** 165117
[39] Pan J S, Li L and Gong J 2021 *Phys. Rev. B* **103** 205425
[40] Lee C H and Longhi S 2020 *Commun. Phys.* **3** 147
[41] Zhou L, Gu Y and Gong J 2021 *Phys. Rev. B* **103** L041404
[42] Lv C, Zhang R, Zhai Z and Zhou Q 2021 arXiv preprint arXiv: 2106.02477
[43] Stålhammar M, Larana-Aragon J, Rødland L and Kunst F K 2022 arXiv preprint arXiv: 2106.05030
[44] Bender C M and Boettcher S 1998 *Phys. Rev. Lett.* **80** 5243
[45] El-Ganainy R, Makris K G, Khajavikhan M, Musslimani Z H, Rotter S and Christodoulides D N 2018 *Nat. Phys.* **14** 11
[46] Stegmaier A, Imhof S, Helbig T, Hofmann T, Lee C H, Kremer M, Fritzsche A, Feichtner T, Klembt S, Höfling S, *et al.* 2021 *Phys. Rev. Lett.* **126** 215302
[47] Fring A 2022 arXiv preprint arXiv: 2201.05140
[48] Xiao L, Deng T, Wang K, Wang Z, Yi W and Xue P 2021 *Phys. Rev. Lett.* **126** 230402
[49] Schomerus H 2013 *Opt. Lett.* **38** 1912
[50] Weimann S, Kremer M, Plotnik Y, Lumer Y, Nolte S, Makris K, Segev M, Rechtsman M C and Szameit A 2016 *Nat. Mater.* **16** 433
[51] Özdemir Ş K , Rotter S, Nori F and Yang L 2019 *Nat. Mater.* **18** 783
[52] Bendix O, Fleischmann R, Kottos T and Shapiro B 2009 *Phys. Rev. Lett.* **103** 030402
[53] Ghatak A, Brandenbourger M, van Wezel J and Coulais C 2020 *Proc. Natl. Acad. Sci. USA* **117** 29561
[54] Xiao L, Deng T, Wang K, Zhu G, Wang Z, Yi W and Xue P 2020 *Nat. Phys.* **16** 761
[55] Bouganne R, Aguilera M B, Ghermaoui A, Beugnon J and Gerbier F 2020 *Nat. Phys.* **16** 21
[56] Song W, Sun W, Chen C, Song Q, Xiao S, Zhu S and Li T 2019 *Phys. Rev. Lett.* **123** 165701
[57] Hou J, Li Z, Luo X W, Gu Q and Zhang C 2020 *Phys. Rev. Lett.* **124** 073603
[58] Longhi S 2018 arXiv preprint arXiv: 1802.05025
[59] Ningyuan J, Owens C, Sommer A, Schuster D and Simon J 2015 *Phys. Rev. X* **5** 021031
[60] Scheibner C, Irvine W T M and Vitelli V 2020 *Phys. Rev. Lett.* **125** 118001
[61] Zeng Q B 2021 arXiv preprint arXiv: 2110.06597
[62] Long Y, Xue H and Zhang B 2021 arXiv preprint arXiv: 2111.02701
[63] Kawabata K and Sato M 2020 *Phys. Rev. Res.* **2** 033391
[64] Aharonov Y, Massar S, Popescu S, Tollaksen J and Vaidman L 1996 *Phys. Rev. Lett.* **77** 983
[65] Nirala G, Sahoo S N, Pati A K and Sinha U 2019 *Phys. Rev. A* **99** 022111
[66] Li J X, Chang S L, Zhao Y H, Xiao X and Leng Y 2021 *Laser Physics* **31** 095202
[67] Martinez Alvarez V M, Barrios Vargas J E and Foa Torres L E F 2018 *Phys. Rev. B* **97** 121401
[68] Okuma N, Kawabata K, Shiozaki K and Sato M 2020 *Phys. Rev. Lett.* **124** 086801
[69] Longhi S 2021 *Phys. Rev. B* **104** 125109
[70] Peng Y, Jie J, Yu D and Wang Y 2022 arXiv preprint arXiv: 2201.10318
[71] Liang Q, Xie D, Dong Z, Li H, Li H, Gadway B, Yi W and Yan B 2022 arXiv preprint arXiv: 2201.09478
[72] Zhu X, Wang H, Gupta S K, Zhang H, Xie B, Lu M and Chen Y 2020 *Phys. Rev. Res.* **2** 013280
[73] Guo C X, Liu C H, Zhao X M, Liu Y and Chen S 2021 *Phys. Rev. Lett.* **127** 116801
[74] Lee C H, Li L, Thomale R and Gong J 2020 *Phys. Rev. B* **102** 085151
[75] Qi X L 2013 arXiv preprint arXiv: 1309.6282
[76] Gu Y, Lee C H, Wen X, Cho G Y, Ryu S and Qi X L 2016 *Phys. Rev. B* **94** 125107
[77] As we interpolate between OBCs and PBCs, we observe a peculiar scaling behavior of the corresponding effective κ.[98]
[78] Guo G F, Bao X X and Tan L 2021 *New J. Phys.* **23** 123007
[79] However, the topological eigenenergies themselves fall outside of the purview of our prescription, because they are isolated solutions that are not adiabatically connected to any Bloch solution.
[80] Ghatak A and Das T 2019 *J. Phys: Condens. Mat.* **31** 263001
[81] Song F, Yao S and Wang Z 2019 *Phys. Rev. Lett.* **123** 246801
[82] Liu H, Zhou J K, Wu B L, Zhang Z Q and Jiang H 2021 *Phys. Rev. B* **103** 224203
[83] Gong Z, Ashida Y, Kawabata K, Takasan K, Higashikawa S and Ueda M 2018 *Phys. Rev. X* **8** 031079
[84] Zhang S B, Denner M M, Bzdušek T, Sentef M A and Neupert T 2022 arXiv preprint arXiv: 2201.12653
[85] Tai T and Lee C H 2022 arXiv preprint arXiv: 2202.03462
[86] Lee C H and Thomale R 2019 *Phys. Rev. B* **99** 201103
[87] Longhi S 2020 *Phys. Rev. Lett.* **124** 066602
[88] Martinez Alvarez V M, Barrios Vargas J E and Foa Torres L E F 2018 *Phys. Rev. B* **97** 121401
[89] Yang R, Tan J W, Tai T, Koh J M, Li L, Longhi S and Lee C H 2022 arXiv preprint arXiv: 2201.04153
[90] Li L and Lee C H 2022 *Science Bulletin* **67** 685
[91] Shen R and Lee C H 2021 arXiv preprint arXiv: 2107.03414
[92] Tahir-Kheli J and Goddard III W A 2011 *The Journal of Physical Chemistry Letters* **2** 2326
[93] Budich J C and Bergholtz E J 2020 *Phys. Rev. Lett.* **125** 180403
[94] Yang X, Li J, Ding Y, Xu M, Zhu X F and Zhu J 2022 *Phys. Rev. Lett.* **128** 065701
[95] Hofmann T, Helbig T, Lee C H, Greiter M and Thomale R 2019 *Phys. Rev. Lett.* **122** 247702
[96] Zou D, Chen T, He W, Bao J, Lee C H, Sun H and Zhang X 2021 *Nat. Commun.* **12** 7201
[97] Blais A, Grimsmo A L, Girvin S M and Wallraff A 2021 *Rev. Mod. Phys.* **93** 025005
[98] Li L, Lee C H and Gong J 2021 *Commun. Phys.* **4** 42
[99] Li L, Lee C H, Mu S and Gong J 2020 *Nat. Commun.* **11** 5491
[100] Liu C H, Zhang K, Yang Z and Chen S 2020 *Phys. Rev. Res.* **2** 043167
[101] Rafi-Ul-Islam S, Siu Z B, Sahin H, Lee C H and Jalil M 2021 arXiv preprint arXiv: 2108.02457